

Short Communication

Laser Pulse Deposited Nanosized Ceria for Direct Electron Transfer of Glucose Oxidase

Mouna Moumene¹, Amel Tabet-Aoul¹, Maxime Gougis¹, Dominic Rochefort², Mohamed Mohamedi^{1,*}

¹Institut National de la Recherche Scientifique (INRS)-Énergie, Matériaux et Télécommunications (EMT), 1650 Boulevard Lionel Boulet, Varennes, Québec, J3X 1S2, Canada.

²Département de Chimie, Université de Montréal, CP 6128 Centre-Ville, Montréal Québec, H3C 3J7, Canada

*E-mail: mohamedi@emt.inrs.ca

Received: 3 September 2013 / Accepted: 14 October 2013 / Published: 15 November 2013

Ceria has a high isoelectric point (IEP~9.2) and its cerium atom reversibly undergoes oxidation/reduction process therefore theoretically capable through electrostatic interactions of immobilizing enzymes with lower IEP and of electrons mediating, respectively. Based on this theoretical bi-functional role, we synthesized nano CeO₂ by pulsed laser deposition on an electrically conductive electrode such as the carbon paper. The direct electron transfer (DET) between both FAD/FADH₂ center of the glucose oxidase (GOx) enzyme and the carbon surface was successfully achieved through the redox centers of CeO₂ located on the electrode surface.

Keywords: Ceria; carbon substrate; glucose oxidase; direct electron transfer; enzyme immobilization; laser ablation.

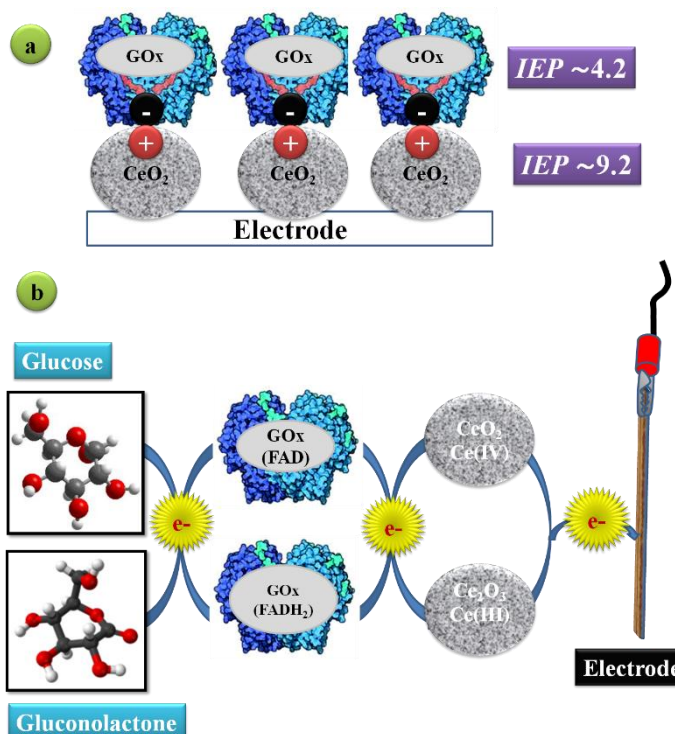
1. INTRODUCTION

Glucose is an important clinical biomolecule for both biosensors and implantable biological fuel cells themselves destined to power several other implantable biomedical devices. The glucose oxidase (GOx) enzymes catalyze glucose electrooxidation at very low electrochemical potentials, making them attractive protein biocatalysts anodes. In order to work as a catalyst, GOx requires a cofactor, flavin adenine dinucleotide (FAD) center that is tightly bound and deeply buried about 15 Å below the protein surface [1]. This center is reduced by glucose to FADH₂. Then FADH₂ is reoxidized to FAD either by molecular O₂, which is reduced to H₂O₂, or by the oxidizing member of a redox couple. However, GOx enzyme is incapable of direct contact with the electrode since its redox center is insulated from the conductive support by the GOx matrice. Establishing direct electron transfer

(DET) with GOx electrodes in which the electrons may jump between the GOx redox center and the electrode constitutes one of the enduring challenges in electrochemical glucose biosensors and electrochemical glucose biofuel cells [2].

Various experimental strategies have been proposed for establishing electrical contacting of GOx with electrodes. These strategies include GOx covalently bound to a reducing potential copolymer that has osmium complexes tethered to its backbone [3], a molecular wire modified glassy carbon electrode [4], GOx covalently wired via viologen to electrically conductive polypyrrole films [5], carbon nanotubes (CNTs)/nafion-based electrodes [6], adsorption of GOx onto electrochemically functionalized CNTs [7], deglycosylation of GOx [8], electrical contacting of GOx in a redox-active rotaxane configuration [9], graphene-based bioelectrodes [10], enzyme immobilized onto reduced graphene oxide/ZnO composite [11], electrochemically preanodized screen-printed carbon electrode [12], covalently linked layers of GOx, CNTs and poly-l-lysine on pyrolytic graphite [13], and amine-terminated ionic liquid functionalized CNT-gold nanoparticles for investigating the DET of GOx [14].

Cerium dioxide (CeO_2) is one of the most actively investigated materials in bioelectrocatalysis and materials applications [15]. Indeed, its low cost, biocompatibility, and low temperature processing make CeO_2 of great interest for a wide range of applications such as oxygen gas sensors, biosensors and biofuel cells. Nevertheless, relatively few applications of nanoceria in bioanalysis have been described. Most recently, nanosized ceria have been found to display superoxide dismutase mimetic activity and catalase mimetic activity [16].



Scheme 1. Concept. (a) GOx immobilization through electrostatic interactions with CeO_2 ; and (b) direct electron transfer process.

Importantly, the high isoelectric point (IEP~9.2) of CeO₂ can be helpful to immobilize an enzyme with low IEP such as GOx (IEP~4.2) [17]. Indeed, the positively charged CeO₂ surface offers a friendly platform for the negatively charged GOx, and the electrostatic interactions between CeO₂ and GOx help to retain the bioactivity of GOx (Scheme 1a). Moreover, CeO₂ has shown a great ability to store and release oxygen with little distortion of the lattice, as the cerium atom reversibly undergoes oxidation/reduction processes from Ce⁴⁺ to Ce³⁺ [18]. Owing to this second property, the network of Ce redox centers is expected to electrically "wires" the reactions center of the protein to the current collector (electrode), which will enhances the rapid electron shuttling with the FAD redox center of GOx (Scheme 1b).

In this work, we report for the first time, the implementation of the concept shown in Scheme 1. Nanosized CeO₂ with a unique morphology was synthesized at room temperature by pulsed laser deposition (PLD) directly onto an electrically conductive carbon paper, CP (current collector) and demonstrates an unprecedented DET between nanosized ceria and GOx protein.

2. EXPERIMENTAL

2.1. Materials synthesis

CeO₂ was synthesized by PLD at room temperature by means of a pulsed KrF excimer laser ($\lambda = 248$ nm, pulse width = 17 ns, and repetition rate = 50 Hz). Pure CeO₂ target (99.99%, Kurt J. Lesker Co.) was used to deposit CeO₂ using a laser fluence of 4 J cm⁻² and 20000 laser pulses under vacuum (4x10⁻⁵ Torr).

2.2. Characterization

The surface morphology of the as-prepared samples was examined by means of a field emission scanning electron microscope (SEM, JEOL, JSM 7401F apparatus) and a transmission electron microscopy (JEOL-JEM-2100F operating at 200 kV).

X-ray photoelectron spectroscopy (XPS) measurements were carried out via a VG Escalab 220i-XL set with an Al K α source (1486.6 eV). A survey spectra ranging from 0 to 1000 eV was acquired. Quantification of the elements was performed with CasaXPS software (Casa Software Ltd.) by fitting the core level spectra after a Shirley background removal

Micro-Raman spectroscopy was performed by using the 514.5 nm (2.41 eV) laser radiation of an Ar⁺ laser with a circular polarization. The laser beam was focused onto the sample to a spot size of 1 μ m in diameter (micro-Raman spectroscopy, Renishaw Imaging Microscope WireTM).

2.3. Enzyme immobilization

GOx was immobilized on CeO₂ by physisorption. To do so, CeO₂ samples were soaked in phosphate buffer solution (PBS, pH=7.2, from Sigma-Aldrich, Canada Ltd.) containing 15mg/mL GOx

from *Aspergillus niger* (168800 units/G Sigma-Aldrich Canada Ltd.) and stored overnight at 4 °C in a refrigerator before use.

2.4. Electrochemical measurements

DET properties between the GOx and the CeO₂ substrates were studied by cyclic voltammetry (CV) in a deaerated phosphate buffer solution (PBS, pH=7.2) with and without glucose solution (D-(+)-Glucose, ACS reagent grade, from Sigma-Aldrich).

All electrochemical measurements were conducted at room temperature using a three-electrode cell with the reference electrode and counter electrode being an Ag/AgCl, 3M NaCl and a platinum coil, respectively. Data were controlled and acquired with a potentiostat/galvanostat Autolab from EcoChemie.

3. RESULTS AND DISCUSSIONS

3.1. Characterisation

The morphology and microstructure of the CeO₂ were examined by field-emission scanning electron microscopy (FESEM) and micro Raman spectroscopy. The FESEM images (Fig. 1 a-c) reveal that the surface of the product is smooth with a topography resembling a jigsaw.

The Raman spectrum of the CP/CeO₂ (Fig. 1d) shows two bands characteristics of the CP substrate, the first order G mode (E_{2g} symmetry) at ~1582 cm⁻¹ ascribed to a regular sp₂ graphitic network, and the D mode (A_{1g} symmetry) at ~1355 cm⁻¹, which reflects the disorder and defects in the carbon lattice [19]. In addition, the spectrum displays a third band at ~455.6 cm⁻¹ with a full width half maximum (FWHM) of 35.3 cm⁻¹ assigned to triply degenerate Raman active F_{2g} mode of CeO₂ [20]. For a bulk CeO₂, the F_{2g} mode is located at ~465.4 cm⁻¹ with a FWHM of 9.5 cm⁻¹ [21]. The red shift and broadening of the phonons in our synthesized ceria is attributed to the formation of nanocrystalline phase for the film [22].

The PLD deposition of CeO₂ induced growth of randomly oriented networked particles, which can be seen by TEM (Fig. 2a). The high-resolution TEM, HR-TEM (Fig. 2b) shows well-defined crystallites with strong faceting and well-defined edges. Most of the nanoparticles have polyhedral shape confirming the presence of randomly-oriented ceria crystallites. The crystal size could be clearly observed and ranged between 2 to 5 nm. The lattice fringes could be observed in magnified images of different crystallites (Fig. 2b insets) and measured to be 1.9 and 3.2 Å, corresponding to the interplane distances between the (220) and (111) lattice planes of cubic CeO₂. The selected-area electron diffraction (SAED) (Fig. 2c) patterns results from a typical polycrystalline structure indicating a fine-grained nanocrystalline film. The reflections are consistent with the cubic phase, as clearly identified by the overlaid Miller indices.

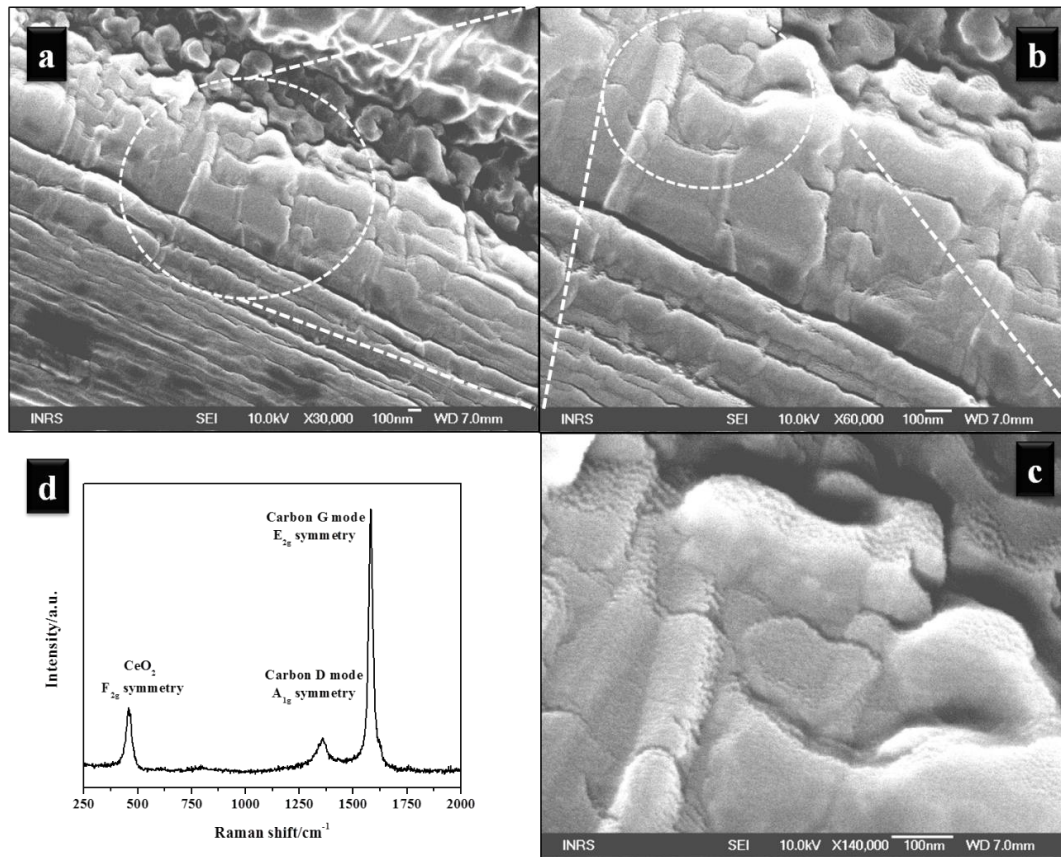


Figure 1. Room temperature PLD-synthesized CeO₂. (a-c) FESEM images at increasing magnification. (d) Raman spectrum of the CeO₂/carbon paper substrate.

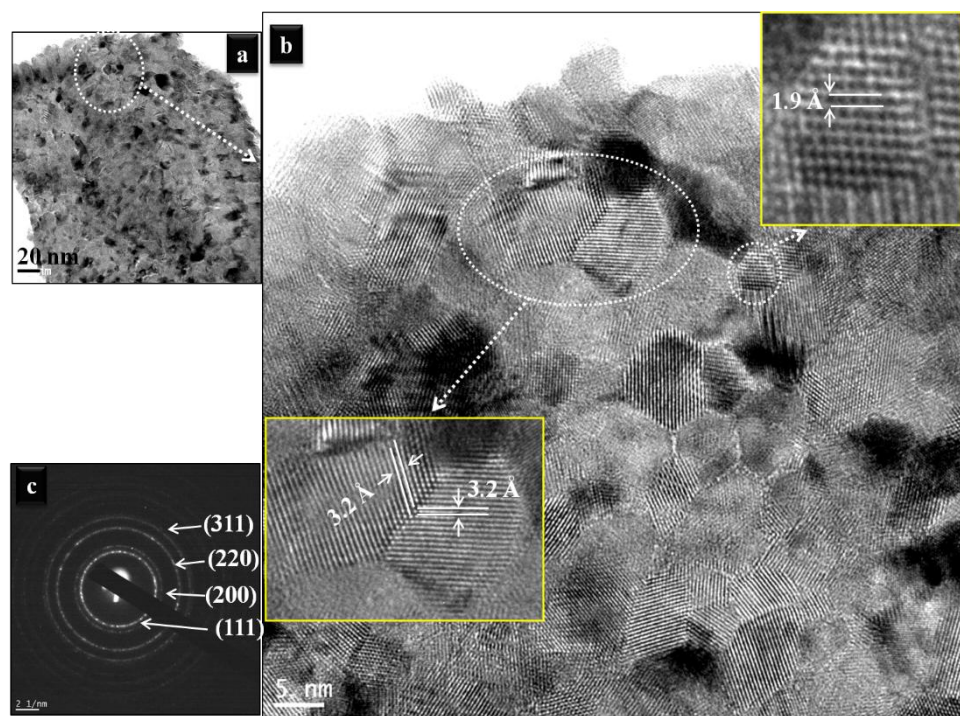


Figure 2. Room temperature PLD-synthesized CeO₂. a-b) HR-TEM images at increasing resolution. c) SAED patterns.

XPS has proven as an effective tool to identify immobilization or adsorption of proteins [23]. Figure 3 compares the wide survey spectra of CP/CeO₂ and CP/CeO₂/GOx. The spectrum of CP/CeO₂ presents peaks only for Ce, C and O with a surface concentration of 16.61, 33.82, and 49.58 at%, respectively. The spectrum of CP/CeO₂/GOx reveals the presence of a new element that is nitrogen with its N 1s corelevel appearing at 400.5 eV. The surface concentration Ce, C, O and N is of 3.33, 59.79, 32.01 and 4.88 at%, respectively. The N 1s band can be ascribed to species where nitrogen is bound to carbon and to functional groups. Thus, the occurrence of nitrogen is a conclusive evidence of the GOx presence in the processed sample.

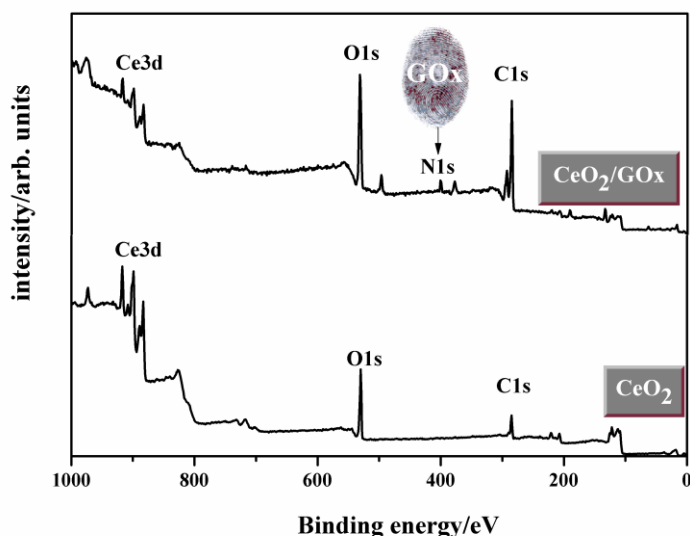


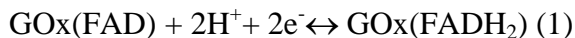
Figure 3. XPS spectra of bare CeO₂ and GOx immobilized onto CeO₂.

3.2. Electrochemistry at CP/CeO₂ and CP/CeO₂-GOx electrodes

Figure 4a compares cyclic voltammograms (CVs) recorded at CP/CeO₂ electrodes within the potential range of -0.6 V to 0.6 V vs. Ag/AgCl in 0.2 M PBS at pH 7.2 without and with 20 mM of glucose. One can observe the presence of a redox couple, Ox₁/Red₁ at ~0.085/0.023 V vs. Ag/AgCl. This redox couple originated from the remaining uncoated carbon paper substrate, i.e., to oxidation/reduction of carbon surface oxide groups preformed by adsorbed ambient oxygen at the surface of CP. We have conducted a control experiment on bare CP in PBS solution and the Ox₁/Red₁ redox waves were confirmed.

Figure 4b compares CVs recorded at CP/CeO₂/GOx in PBS and in 20 mM glucose + 0.2 M PBS at pH 7.2, under anaerobic conditions. The CV in the absence of glucose was performed to elucidate if GOx immobilized on CeO₂ surface can undergo DET with the electrode. The CV of CP/CeO₂/GOx in PBS solution shows the presence of an oxidation (Ox₂) and reduction (Red₂) waves at -0.444 V and -0.482 V vs Ag/AgCl, respectively, which gives a formal potential of -0.463 V vs Ag/AgCl. This value is very close to the FAD/FADH₂ redox potential under physiological pH

[24]. Thus the redox waves observed at -0.444/-0.482 V vs. Ag/AgCl in the absence of glucose can be confidently considered as a result of the redox reaction of the active site of GOx immobilized on the surface of the CeO₂ corresponding to the conversion between GOx(FAD) and GOx(FADH₂) according to Eq. (1) [25]:



It can be concluded that the redox process obtained with CP/CeO₂/GOx in the absence of glucose indicate that electrical communication between the redox center of GOx and carbon paper has been provided through the CeO₂ located on the electrode surface. Thus, the DET of GOx at CP/CeO₂ film has been achieved successfully.

In the presence of glucose (Fig. 4b, blue curve), the redox waves become more visible and peak shaped centered around at -0.433 V (Ox₂) and -0.480 V (Red₂) which provides a formal potential of ca -0.456 V. The peak-to-peak separation ratio of cathodic to anodic current intensity is as small as ~47 mV, revealing a fast electron transfer process. Furthermore, the current increased in the presence of glucose, which demonstrates the ability of GOx to simultaneously undergo DET with the electrode and retains biocatalytic activity. Thus, when glucose is added, the formation of FADH₂ occurs in the vicinity of the electrode surface following Eq. (2):

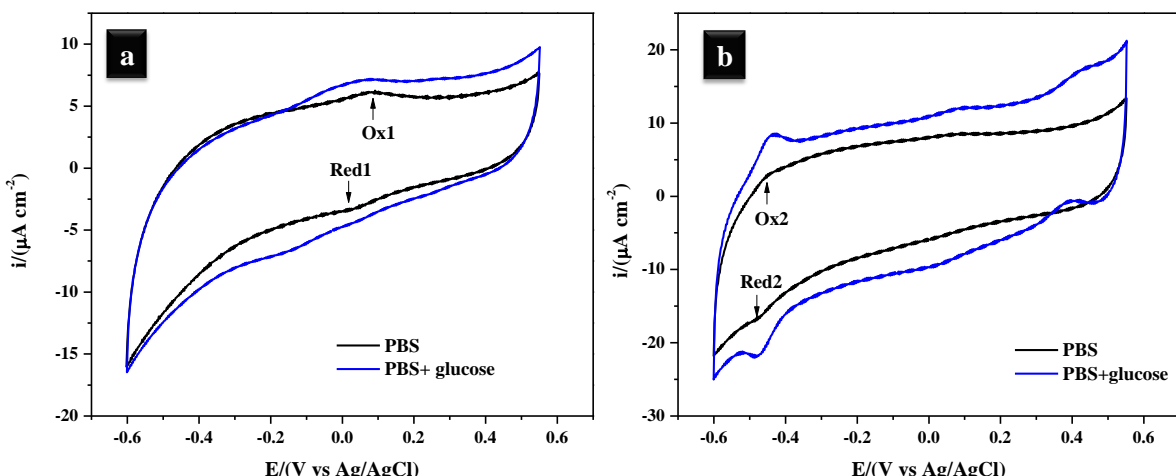


Figure 4 Cyclic voltammetry with 100 mV s⁻¹ scan rate run in 0.2 M PBS at pH 7.2 without and with 20 mM of glucose at a) CP/CeO₂ and b) CP/CeO₂/GOx electrodes.

4. CONCLUSIONS

In this study, we demonstrate the synthesis and use of nanosized ceria as a potential candidate for bringing out the DET. These results will contribute to the development of important research areas such as enzymatic glucose biofuel cells and enzymatic glucose electrochemical sensors. A full study is

planned to investigate the effect of various morphologies of CeO₂ films (smooth surface vs porous surface) and of various thicknesses (mono to multi-layers) not only on the DET process but also on glucose electrooxidation. Such systematic study will shed light on the promotional effect of Ceria to GOx enzyme with respect to DET process and glucose electro-oxidation reaction.

ACKNOWLEDGEMENT

This work was financially supported by the Natural Sciences Engineering Research Council of Canada (NSERC), the Fonds Québécois pour la Recherche en Nature et Technologie (FQRNT).

References

1. G. Wohlfahrt, S. Witt, J. Hindle, D. Schomburg, H. M. Kalisz, H.-J. Hecht, *Acta Crystallogr. Sect. D*, 55 (1999) 969.
2. J. Liu, A. Chou, W. Rahmat, M. N. Paddon-Row, J. J. Gooding, *Electroanalysis*, 17 (2005) 38.
3. T. Chen, S. C. Barton, G. Binyamin, Z. Gao, Y. Zhang, H.-H. Kim, and A. Heller, *J. Am. Chem. Soc.*, 123 (2001) 8630.
4. G. Liu, M. N. Paddon-Row, J. J. Gooding, *Electrochim. Comm.*, 9 (2007) 2218.
5. X. Liu, K. G. Neoh, L. Cen, E. T. Kang, *Biosens. Bioelectron.*, 19 (2004) 823.
6. J. Wang, M. Musameh, Y. H. Lin, *J. Am. Chem. Soc.*, 125 (2003) 2408.
7. M. Moumene, D. Rochefort, M. Mohamedi, *Int. J. Electrochem. Sci.*, 8 (2013) 2009.
8. O. Courjean, F. Gao, and N. Mano, *Angew. Chem. Int. Ed.*, 48 (2009) 5897.
9. E. Katz, L. Sheeney-Haj-Ichia, and I. Willner, *Angew. Chem. Int. Ed.*, 43 (2004) 3292.
10. B. Devadas, V. Mani, S.-M. Chen, *Int. J. Electrochem. Sci.*, 7 (2012) 8064.
11. S. Palanisamy, A.T. Ezhil Vilian, S.-M. Chen, *Int. J. Electrochem. Sci.*, 7 (2012) 2153.
12. Ting-Hao Yang, Chi-Lung Hung, Jyh-Harng Ke, Jyh-Myng Zen, *Electrochim. Comm.*, 10 (2008) 1094.
13. Abhay Vaze, Nighat Hussain, Chi Tang, Donal Leech, James Rusling, *Electrochim. Comm.*, 11 (2009) 2004.
14. Ruifang Gao, Jianbin Zheng, *Electrochim. Comm.*, 11 (2009) 608.
15. Bin Zhu and Mahmut D. Mat, *Int. J. Electrochem. Sci.*, 1 (2006) 383; Xiao Wang, Dapeng Liu, Shuyan Song and Hongjie Zhang, *Chem. Commun.*, 48 (2012) 10207; L. He, F. J. Yu, X. B. Lou, Y. Cao and N. Fan, *Chem. Commun.*, 46 (2010) 1553; T. Mitsudome, Y. Mikami, M. Matoba, T. Mizugaki, K. Jitsukawa, and K. Kaneda, *Angew. Chem. Int. Ed.*, 51 (2012) 136.
16. T. Pirmohamed, J. M. Dowding, S. Singh, B. Wasserman, E. Heckert, A. S. Karakoti, J. E. S. King, S. Seal and W. T. Self, *Chem. Commun.*, 46 (2010) 2736.
17. P. R. Solanki, C. Dhand, A. Kaushik, A. A. Ansari, K. N. Sood, B. D. Malhotra, *Sens. Actuators B*, 141 (2009) 551.
18. S. Deshpande, S. Patil, S. V. N. T. Kuchibhatla, S. Seal, *Appl. Phys. Lett.*, 87 (2005) 133113.
19. M. S. Dresselhaus, G. Dresselhaus, R. Saito, A. Jorio, *Phys. Rep.*, 409 (2005) 47.
20. J. E. Spanier, R. D. Robinson, F. Zhang, S.-W. Chan, and I. P. Herman, *Phys. Rev. B*, 64 (2001) 245407.
21. I. Estrela-Lopis, G. Romero, E. Rojas, S. E. Moya and E. Donath, *J. Phys.: Conf. Ser.*, 304 (2011) 012017.
22. Y. Zhang, P. D. Edmondson, T. Varga, S. Moll, F. Namavar, C. Lan and W. J. Weber, *Phys. Chem. Chem. Phys.*, 13 (2011) 11946.
23. D. Ivnitski, K. Artyushkova, R. A. Rincón, P. Atanassov, H. R. Luckarift, and G. R. Johnson, *Small*, 4 (2008) 357.

24. D. Ivnitski, B. Branch, P. Atanassov, C. Apblett, *Electrochem. Comm.*, 8 (2006) 1204.
25. R. Ianniello, J. Lindsay, A. Yacynych, *Anal. Chem.*, 54 (1982) 1098.